Biosensors and Bioelectronics 241 (2023) 115667

Contents lists available at ScienceDirect

Biosensors and Bioelectronics

journal homepage: www.elsevier.com/locate/bios

High-sensitivity hemoglobin detection based on polarization-differential spectrophotometry

Chunlan Deng [a,c,1], Qilai Zhao [b,c,*,1], Yichuan Gan [d], Changsheng Yang [c,f,i], Hongbo Zhu [e], Shiman Mo [a,c], Junjie Zheng [b,c], Jialong Li [b,c], Kui Jiang [a,c], Zhouming Feng [a,c], Xiaoming Wei [b,c], Qinyuan Zhang [b,c,f,g], Zhongmin Yang [b,c,f,g,h], Shanhui Xu [a,b,c,f,g,h,i,**]

[a] School of Materials of Science and Engineering, South China University of Technology, Guangzhou, 510640, China
[b] School of Physics and Optoelectronics, South China University of Technology, Guangzhou, 510640, China
[c] State Key Laboratory of Luminescent Materials and Devices and Institute of Optical Communication Materials, South China University of Technology, Guangzhou, 510640, China
[d] The Third Affiliated Hospital of Southern Medical University, Guangzhou, 510630, China
[e] State Key Laboratory of Luminescence and Applications, Changchun Institute of Optics, Fine Mechanics and Physics, Chinese Academy of Sciences, Changchun, 130033, China
[f] Guangdong Engineering Technology Research and Development Center of Special Optical Fiber Materials and Devices, Guangzhou, 510640, China
[g] Guangdong Provincial Key Laboratory of Fiber Laser Materials and Applied Techniques, South China University of Technology, Guangzhou, 510640, China
[h] Guangdong Engineering Technology Research and Development Center of High-performance Fiber Laser Techniques and Equipments, Zhuhai, 519031, China
[i] Hengqin Firay Sci-Tech Company Ltd., Zhuhai, 519031, China

ARTICLE INFO

Keywords:
Spectrophotometry
Polarization difference
Hemoglobin
High-sensitivity
Single-frequency fiber laser

ABSTRACT

Hemoglobin content is recognized as a momentous and fundamental physiological indicator, especially the precise detection of trace hemoglobin is of great significance for early diagnosis and prevention of tumors, cancer, organic injury, etc. Therefore, high-sensitivity hemoglobin detection is imperative. However, effective detection methods and reliable detection systems are still lacking and remain enormous challenges. Herein, we present a synthetical strategy to break through the existing bottleneck based on polarization-differential spectrophotometry and high-performance single-frequency green fiber laser. Importantly, this framework not only has precisely extracted the two-dimensional information of intensity and polarization during the interaction between laser and hemoglobin, but also has taken advantage of the high monochromaticity and fine directivity in the optimized laser source to reduce the undesirable scattered disturbance. Thus, the hemoglobin detection sensitivity of 7.2×10^{-5} g/L has advanced a hundredfold compared with conventional spectrophotometry, and the responsive dynamic range is close to six orders of magnitude. Results indicate that our technology can realize high-sensitivity detection of trace hemoglobin content, holding promising applications for precision medicine and early diagnosis as an optical direct and fast detection method.

1. Introduction

Hemoglobin (Hb) is a kind of significant protein in red blood cells from higher organisms (Pillai et al., 2020). This protein has consisted of one globin and four heme centers, acting as a carrier that mainly transports molecular oxygen from the lungs to the rest organs and tissues in the body (Zhao et al., 2017). The disorder of the Hb concentration can be related to various diseases such as anemia (Pasricha et al., 2021), leukemia (Kalluri and LeBleu, 2020), diabetes (Jian and Felsenfeld, 2021), perivascular disease (Månberg et al., 2021), etc. Furthermore, compared with the high concentration of Hb analysis in the blood test, trace Hb detection is also purposeful in clinical diagnoses such as hemoglobinuria (Zhou et al., 2021) and fecal occult blood (Mimee et al., 2018), which may be the sign of tumor (Dell'Olio et al., 2021), and cancer (Das et al., 2016), even related to gene mutation (Kowalczyk et al., 2019).

* Corresponding author. School of Physics and Optoelectronics, South China University of Technology, Guangzhou, 510640, China.
** Corresponding author. School of Materials of Science and Engineering, South China University of Technology, Guangzhou, 510640, China.
E-mail addresses: zhaoql@scut.edu.cn (Q. Zhao), flxshy@scut.edu.cn (S. Xu).
[1] These authors contributed equally.

https://doi.org/10.1016/j.bios.2023.115667
Received 4 May 2023; Received in revised form 28 July 2023; Accepted 3 September 2023
Available online 9 September 2023

Nowadays, many methods have been attempted for Hb detection (Baugh et al., 2017), including fluorescent analysis (Tenner et al., 2021), electrochemical analysis (Suhito et al., 2022), spectrophotometry (Wyatt et al., 1986), and so on. Fluorescent analysis and electrochemical analysis respectively utilize fluorescent signals (Dai et al., 2017) and electrochemical signals (Ryu et al., 2016) for Hb detection with some biochemical (Amiri et al., 2021) and physical treatment (Eissa and Zourob, 2017) of the blood sample, which are cumbersome and time-consuming (Han et al., 2019). As an optically direct detection method, spectrophotometry is performed by detecting monochromatic light intensity variation caused by the absorption of Hb or its derivatives based on the Lambert-Beer law (Vlk et al., 2021). Until now, toxic chemical reagents (Heil et al., 2021) in traditional spectrophotometry are gradually replaced by nontoxic ones or even unnecessary (Passos et al., 2019), and the detection light source also substitutes with light emitting diode (LED) (Shuhang et al., 2022) and laser diode (LD) (Ra et al., 2020). As a result, a lower limit of detection (LLOD) (Huang et al., 2013) of 1.85×10^{-3} g/L (Fiedoruk-Pogrebniak et al., 2018) is realized. However, the detection sensitivity is still limited by the light source with slightly poor stability, monochromaticity and directionality.

In recent years, some other detection methods based on optical principles, such as photoacoustic spectrometry (Arslanov et al., 2012), dynamic spectrometry (Dremin et al., 2019) and spectral imaging method (Sereda et al., 2013) has also attracted much attention of researchers. Photoacoustic spectrometry applies the quantitative relationship between the strength of the photoacoustic signal and Hb concentration to detection. The process is easy to operate, but the photoacoustic signal is weak and easily drowned by noise. Dynamic spectrometry is based on photoplethysmography signals in subcutaneous vessels to realize detection. However, the optical properties of skin are complex, which may lead to unstable detection results. The spectral imaging method utilizes the spectral characteristics of the detection site to carry on the imaging analysis, but the instrument of this imaging method is complex and has high requirements for the detection site. These methods explore extensive information on the interaction between biology and light from different dimensions, and can realize the non-invasive and real-time detection of Hb. However, their sensitivity, accuracy, and stability are vulnerable to adverse effects due to much interference during detection.

Considering all these factors, we present a new method to combine intensity variation and polarization difference for Hb detection, polarization-difference spectrophotometry, whose contribution is more than simply pooling their efforts together. Besides, a self-made green single-frequency fiber laser (SFFL) with excellent monochromaticity and directionality is used as the detection laser source, whose linear polarization performance is further adjusted by the spatial element, and then interacts with the above sample. By detecting the combined value of intensity change and polarization difference of the laser emitted from the sample, i.e., polarization-differential absorbance (PDA), and analyzing the correlation between PDA and Hb concentration, the following results are finally obtained. The responsive dynamic range of the above samples covered nearly six orders of magnitude with the LLOD 7.20×10^{-5} g/L, and the mean relative error (MRE) of Hb test value from the volunteers is 3.19%. The results indicate that the detection accuracy and sensitivity are both excellent, which can be applied to early diagnosis of diseases, and rapid detection (<10 ms) also has advantages in reducing detection duration.

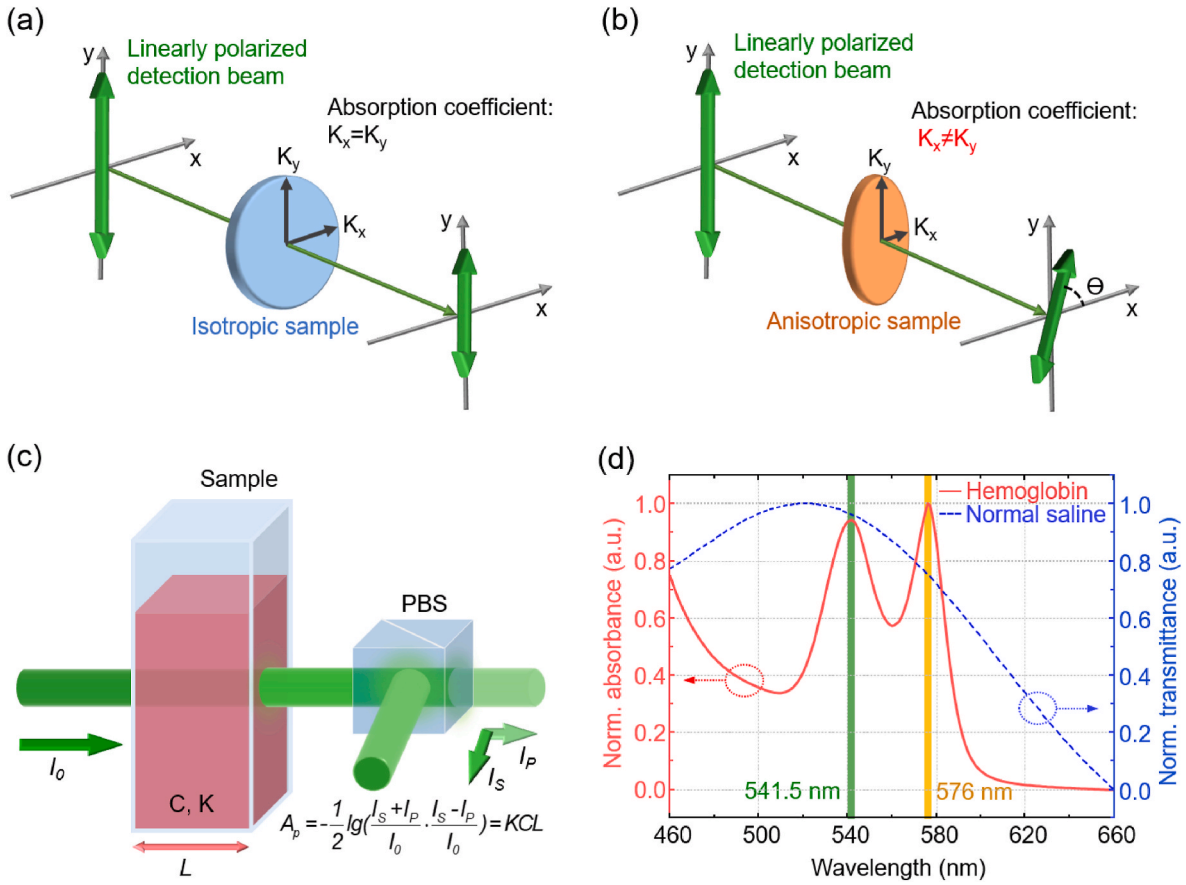

Fig. 1. Comprehensive optimization of Hb detection strategy. Effects of (a) isotropic and (b) anisotropic absorption on linearly polarized detection light. (c) Schematic diagram of polarization-differential spectrophotometry. (d) Absorption spectrum of Hb and transmission spectrum of normal saline in the wavelength range of 460 nm–660 nm.

2. Material and methods

2.1. Main idea

Fig. 1 (a) and (b) briefly reveal the effects of isotropic and anisotropic absorption on linearly-polarized detection beams, respectively. Hb exhibits anisotropy macroscopically owing to the nonuniform and discontinuous arrangement of its various microscopic particles. Because the absorption coefficient of anisotropic medium is different in vertical and horizontal polarized directions ($K_x \neq K_y$), the intensity change and the polarization plane rotation of the detection light is induced together, while the absorption by anisotropic medium only changes the former. The rotation angle arising from anisotropic absorption is proportional to concentration of the substance within a certain range, which is called polarimetry (He et al., 2021) and can be used for quantitative analysis. Regrettably, similar to spectrophotometry with single-dimensional information about light intensity, polarimetry only utilizes polarization information, which limits the sensitivity and accuracy of detection. In addition, some studies (Mu et al., 2012) utilize polarization-differential two-dimensional information to reduce undesirable disturbance and enhance detection sensitivity to realize detection of substance content or distribution, which also gives us some new ideas.

Consequently, as shown in Fig. 1(c), we introduce polarization-differential spectrophotometry to precisely extract the two-dimensional information of intensity and polarization difference during the interaction between light and Hb. The combination of absorbance and polarization difference can reduce undesirable disturbances in the detection process (Venables et al., 2022). Specifically, the polarization-differential factor $(I_S\text{-}I_P)/I_0$ and the conventional absorbance $A=\text{-}lg\{(I_S + I_P)/I_0\}$ are combined and corrected to obtain the expression for PDA (A_p):

$$A_p = -\frac{1}{2}\lg\left(\frac{I_S + I_P}{I_0}\cdot\frac{I_S - I_P}{I_0}\right) = KCL \tag{1}$$

where I_0 is the incident beam intensity, I_S and I_P is the transmitted beam intensity in vertical and horizontal polarized directions, respectively, K is the absorption coefficient, C is the concentration of the analyte, and L is the thickness of the analyte. Eq. (1) reveals that the concentration of the analyte is proportional to PDA when the incident light and the analyte are stable, which can be used as a quantitative analysis of the Hb detection (Veenstra et al., 2019). This method can not only enhance the information extraction of the interaction effect between Hb and light to advance the sensitivity, but also eliminate the disturbance influence from the isotropic impurities to boost the accuracy.

In addition to the above optimization of the detection method, next strategy is to enhance the performance of the detection light source. Affected by the molecular structure of Hb, whose autochrome group results in redshift of absorption spectrum in the ultraviolet band (Miao et al., 2021), it absorbs yellow-green light strongly (Kim et al., 2005). Hb absorption and transmission spectrum from 460 to 660 nm wavelength ranges are described in Fig. 1(d), and there are two strong absorption peaks at 541.5 nm (green light) and 576 nm (yellow light). Compared with yellow light, the transmittance of green light in water (Langford et al., 2001) or normal saline (Lee et al., 2013) is more excellent, so water or normal saline used to dilute the blood sample also has less or negligible disturbance for Hb detection. Besides, the penetrability of the light source in the medium is closely related to its monochromatism and directionality, and its optimization can effectively suppress biological scattering. Therefore, rather than continuing the use of LED or LD, we adopt a 1 μm SFFL along with the waveguide-mode second-harmonic generation method to produce an ideal light source for Hb detection. It has favorable monochromaticity and directionality, meanwhile, more details are given in the next part.

2.2. Experimental program design

The experimental setup of the Hb detection is depicted in Fig. 2(a), which consists of a laser source and a detection unit. The laser source includes linearly-polarized single-frequency seed laser, polarization-maintaining fiber amplifier, and second-harmonic generator. The structure schematic diagram of the laser cavity is shown in Fig. 2(b), based on a self-made Yb^{3+}-doped phosphate fiber (YPF) (Xu et al., 2011), a distributed Bragg reflector (DBR) SFFL with a central wavelength of 1083 nm is used as the seed laser. Then the power of the seed laser is increased to exceed the threshold of second-harmonic generation via the fiber amplifier, and a band-pass filter (BPF) at the end of the fiber amplifier is used to filter out stray light and further improve monochromaticity. Relevant techniques can be found in our previous work (Zou et al., 2009). Periodically poled $LiNbO_3$ waveguide (PPLN WG), as the second-harmonic generation device, is chosen for obtaining 541.5 nm laser, whose all-fiber structure is beneficial to stable performance. Fig. 2(d) is an object picture of the 541.5 nm laser output spot after the PPLN WG.

Then, the green laser is perfectly collimated output to reduce divergence with distance, and further promote directionality. After passing through a rotatable half-wave plate (HWP) and a rotatable linear polarizer (LPOL), the polarization direction of the aforementioned 541.5 nm laser is corrected, resulting in a satisfactory vertically linearly polarized beam. Then it is divided into the reflected beam and the transmitted beam by a non-polarizing beam splitter (NPBS). The reflected beam is used as the reference light, which is real-time monitored by the first photodetector (PD_1) to reduce the adverse effect of the weak fluctuation in optical power. As the detection light, the transmitted light vertically irradiates the medical cuvette containing the blood sample. Then the outgoing light beam is divided into two light beams in the vertical direction (S) and the horizontal direction (P) through a PBS, which are received by PD_2 and PD_3, respectively. The optoelectronic signals originated from three PDs transmitted to a high-precision data acquisition board with four channel A/D converter of 24-bit resolution (NI PXIe-4464), and how to obtain the value of PDA in Eq. (1) can be seen in Fig. 2(e) for the schematic diagram of signal processing. Finally, all signals are real-time monitored, processed, and analyzed through the computer chassis with the LabVIEW program. The physical diagram of light source and Hb detection device is shown in Fig. 2(c). The size of the whole machine including light source, detection device, and signal processing device is 18 × 16 × 12 inches, which has the potential for miniaturization by designing integrated circuits and nesting optical structures.

2.3. Experimental detection steps

Polarization-differential spectrophotometry is conducted by combining polarization difference and absorbance based on traditional spectrophotometry, whose detection steps are described in detail as follows:

(1) After the detection beam passes through pure normal saline (The blank control sample), the intensity of the transmitted light is tested as I_1 ($I_1 = I_{S1} + I_{P1}$, I_{S1} and I_{P1} are S and P beam intensity of the transmitted light, respectively). The reference beam intensity is recorded as I_2 synchronously. A_P of the blank control sample can be regarded as 0, so I_1 can be used as the initial intensity of the reference beam. Then the proportional coefficient $K = I_1/I_2$ is obtained, which is used to correct the error caused by the fluctuation of the reference beam.

(2) The pure normal saline is changed into the blood dilution sample, and then the transmitted light intensity I_3 ($I_3 = I_{S3} + I_{P3}$) and the reference light intensity I_4 are measured synchronously, and then the real-time value $I_5 = I_4 \cdot K$ of the initial light intensity was obtained.

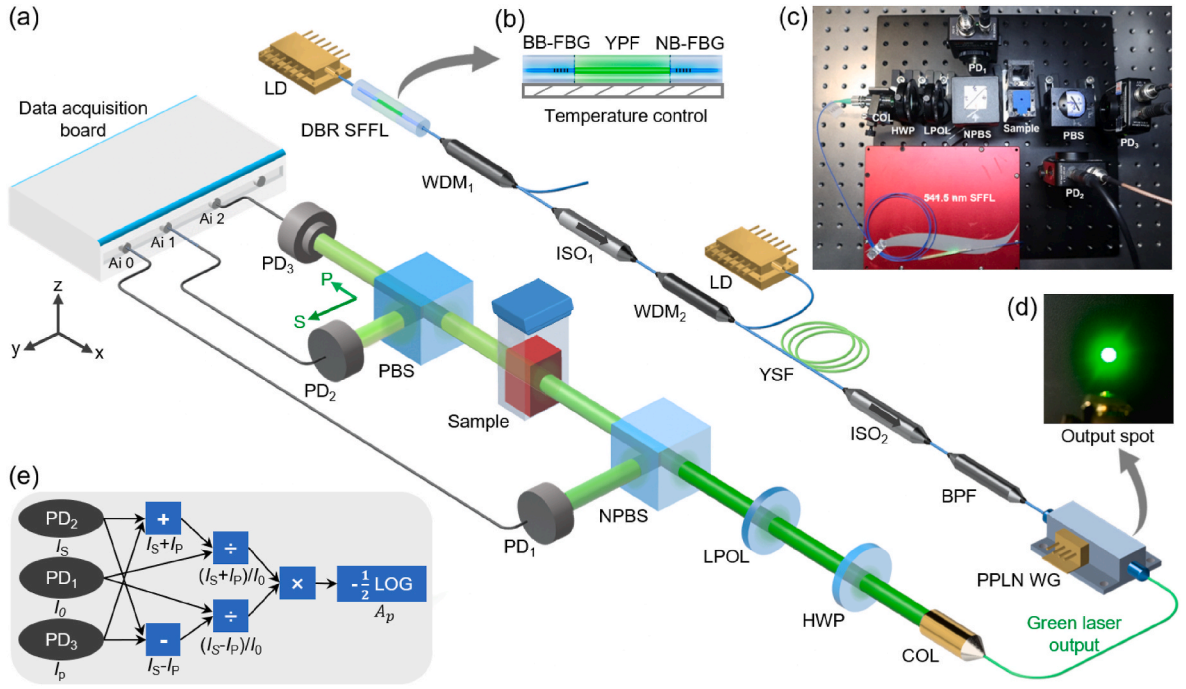

Fig. 2. Experimental setup of Hb detection (not to scale). (a) Main device diagram (LD: laser diode; DBR: distributed Bragg reflector; YPF: Yb^{3+}-doped phosphate fiber; BB: broadband; FBG: fiber Bragg grating; NB: narrowband; PM: polarization-maintaining; ISO: isolator; WDM: wavelength division multiplexer; YSF: Yb^{3+}-doped silica fiber; BPF: band-pass filter; PPLN WG: periodically poled $LiNbO_3$ waveguide; COL: collimator; HWP: half-wave plate; LPOL: linear polarizer; NPBS: non-polarizing beam splitter; PBS: polarizing beam splitter; PD: photodetector). (b) The structure schematic diagram of the laser cavity. (c) Physical diagram of light source and Hb detection device. (d) Object pictures of the 541.5 nm laser output spot after the PPLN WG. (e) Schematic diagram of signal processing.

(3) Finally, PDA is obtained via $A_p = -\frac{1}{2}\lg\left(\frac{I_{S3}+I_{P3}}{I_5}, \frac{I_{S3}-I_{P3}}{I_5}\right)$.

All the above laser intensity values are substituted with the average value (average count 50, sampling rate 5000 Sa/s) of proportional voltage, which is processed by four channel data acquiring board and controlled by the LabVIEW program of the aforementioned experimental device part.

To ensure smooth operation of the Hb detection, it should be noted that: (1) The detected laser power should not be too high to ensure the integrity of the experimental sample, and the low-level laser of less than 5 mW can fully meet the requirements. (2) The cuvette used to hold samples must be selected in advance to ensure the uniformity of quality and light absorption. (3) It should be noted that since the detection light is visible, all detection processes need to be shielded. Otherwise, natural light will adversely affect the detection results. (4) To eliminate the adverse effect of its dark current, the background of the PD needs to be deducted before detection. (5) The environment's temperature and humidity of the entire detection system are better to kept unchanged.

2.4. Reagent and material

The normal saline (Lefeke) is standard 0.9% NaCl solution to dilute blood samples. The normal saline and blood sample are shifted by pipette guns (DragonLab, 0.01 mL, and 0.1 mL model). All samples to be tested are injected into cuvettes (Thermo Fisher, 4.5 mL model, 10 mm optical path) for corresponding experiments, which have Fisher-injectable silicone cover to prevent sample pollution. To configure testing samples at different concentrations, blood samples are accurately and gradually diluted by the gradient dilution method. These blood samples experience no additional processing beyond dilution.

The fiber-based components include LD (Lumentum, S27 Series, 460 mW output power), SFFL (Self-made), WDM (Advanced Fiber Resources (AFR), 980/1083 nm, crystal type), ISO (AFR, 1083 nm, isolation: 39 dB), BPF (AFR, 1083 nm, 3 dB bandwidth: 1 nm), PPLN WG (HC Photonics, 1 × 1 model 541.5 nm), and COL (AFR, 1083 nm, Minimum spot diameter: 0.25 mm). These components are connected into a whole by the polarization-maintaining fiber fusion machine (Fujikura, FSM-100P). The spacial components include HWP (Daheng Optics (DHC), GCL-0605, liquid crystalline polymers material), LPOL (DHC, GCL-0510, Silver nanoparticles film material), NPBS (Edmund Optics, 50:50), PBS (DHC, GCC-4020, Polarized extinction ratio>33 dB), and PD (Thorlabs, PDA100A2, 3 dB bandwidth: 11 MHz). These devices are fixed to an optical platform by an optical bench and screws.

3. Result and discussion

3.1. System performance testing

The monochromatic and directionality of the laser source will directly affect the sensitivity and accuracy of the detection of the Hb (Epah et al., 2022). Monochromaticity can be demonstrated via laser linewidth and spectral purity, and directionality can be represented through beam quality. As shown in Fig. 3(a), a sharp unimodal spectrum with a center wavelength of 541.5 nm is presented, and there is no other stray light. The inset is a 1.90 kHz linewidth result via the self-heterodyne method, indicating the favorable monochromaticity of this laser source. From Fig. 3(b), the beam quality of the laser is $M_x^2 = 1.01$, $M_y^2 = 1.03$, which is near the diffraction limit, and the spot diameter of beam waist after collimation is only about 300 μm with a working distance of 50 mm. Combined with the uniform and symmetrical spot cross-section, it means that the laser source has extraordinary directionality. Moreover, the stability of the laser system is also critical for the reliability and consistency of experimental detection.

Fig. 3(c) shows the power stability and polarization extinction ratio (PER) stability of the 541.5 nm laser system. Power instability in 2 h is less than ±0.61%, indicating that the laser has exceedingly good performance on optical intensity. A PER>31 dB with an instability of less than ±0.57%@2 h also means excellent and stable linear polarization

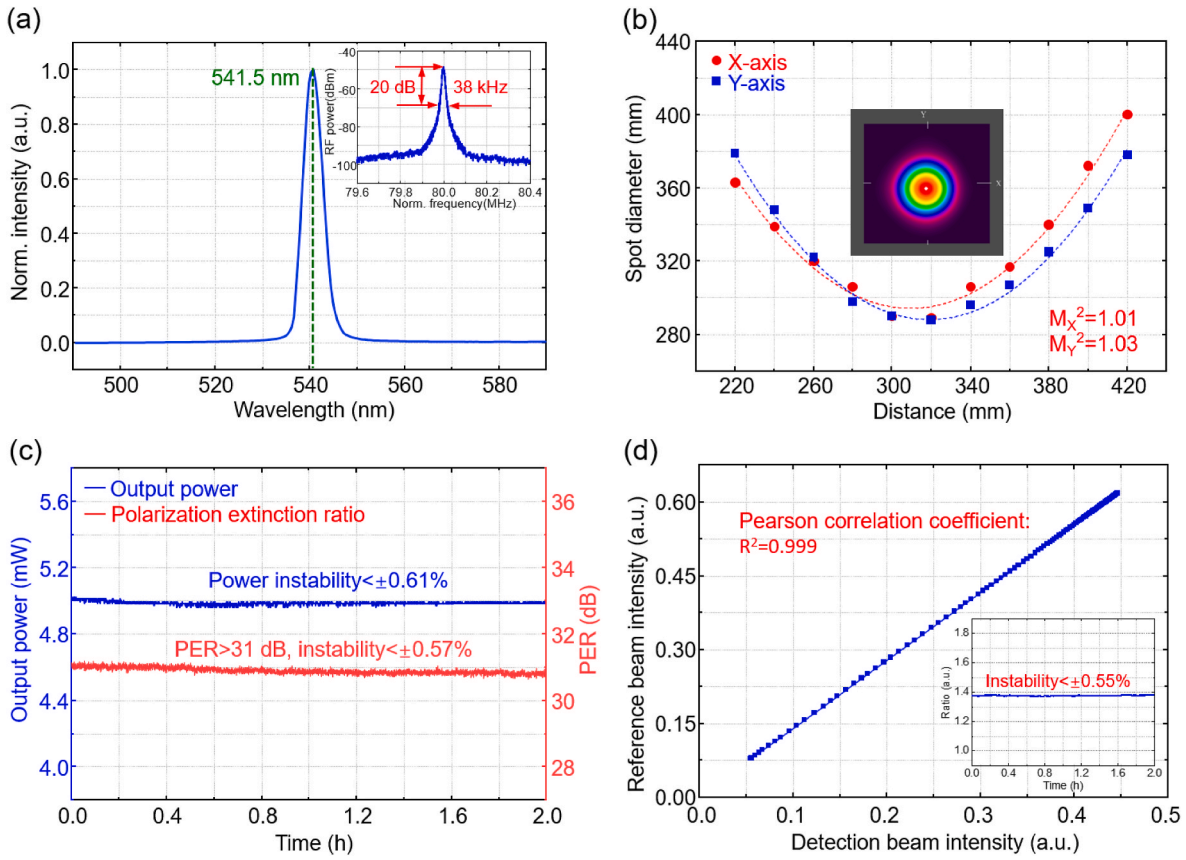

Fig. 3. Specifications of 541.5 nm laser system. (a) Output spectrum. The inset is testing result of linewidth. (b) Beam quality. The inset is energy distribution diagram at the waist. (c) Output power and PER stability. (d) Synchronization of reference beam and detection beam. The inset is the ratio stability of the above two.

characteristic, which is helpful to improve the sensitivity of detection. Furthermore, the reference beam is used to eliminate the adverse effects of optical power fluctuations, so it is essential to ensure that the fluctuations of the reference beam are consistent with that of the detection beam. Synchronicity is shown in Fig. 3(d), whose Pearson correlation coefficient is up to 0.999, and the inset image reflects a $<\pm 0.55\%$ fluctuation in the ratio of the above two beams in 2 h. The synchronism of intensity fluctuations of the detection beam and the reference beam ensures the accuracy of the subsequent detection.

3.2. Hb detection results

Before the formal detection, the PDs need to be corrected by deducting the dark current. Subsequently, the blank control sample (pure normal saline) is beforehand measured, and PDA of the blank control sample can be regarded as 0. Then, the intensity ratio of the detection beam and the reference beam is recorded in advance, as a conversion factor, which can accurately obtain the real-time intensity of the detection beam. Finally, by testing the biological samples and extracting the optoelectronic signals of three PDs via PDA from Eq. (1), the Hb content can be precisely acquired.

The venous blood of healthy volunteers is used in these subsequent experiments. All steps involving biological samples are performed in collaboration with The Third Affiliated Hospital of Southern Medical University. Before configuring these samples, we need to test the original Hb concentration (Mindray BC-6800Plus) of the blood samples (the blood of the same sample group is taken from the same volunteer and sampled in the same time period), and use this test value as the initial value for the subsequent configuration of the samples for concentration conversion. As can be seen from Fig. 4(a), there are 24 samples diluted by normal saline in total to be detected, which can be divided into 8 groups according to the concentration after dilution (all units are g/L): (1) 14.4×10^1, 7.2×10^1, 3.6×10^1; (2) 14.4, 7.2, 3.6; … …; (8) 14.4×10^{-6}, 7.2×10^{-6}, 3.6×10^{-6}. Although the samples in the last four groups appeared to be transparent, they still contain blood cells and free Hb. In normal saline, red blood cells can maintain a normal form and only very few Hb free naturally, which is equivalent to no damage to the blood sample. Parenthetically, blood samples will maintain activity and no significant change in Hb content in normal saline for a longer period of time if properly preserved (Yakushiji et al., 2021), which will be supported by subsequent experimental data.

As shown in Fig. 4(b), we use commercial LED and our homemade SFFL with the same power (3 mW) and the same collimation effect (the spot size is the same at the same position before incidence) as the light source to incident the same normal saline dilution sample. Compared with the transmission image of LED, it is obvious that the scattering angle of SFFL in the sample is smaller, and the spot of the front view is also smaller and brighter, which verifies the excellent performance of SFFL as the light source and reduction of adverse effects on biological scattering.

It should be added that the detection results of each sample are almost instantaneously acquired (<10 ms), but they are usually based on average values of all data collected by the LabVIEW program in about 1 s for accuracy. Fast detection speed usually means high detection efficiency, which can result in significant savings in detection time in the case of a large number of samples.

Fig. 4(c) illustrates the Hb concentration curves calibrated by venous blood diluted samples in normal saline. It can be seen that the detection ranges from 3.60×10^{-1} g/L to 1.44×10^{-4} g/L meets satisfactory linear fitting (Correlation coefficient $R^2 = 0.972$). Thanks to improving the detection strategy and optimizing the laser source, the detection linear range has achieved nearly four orders of magnitude, which is expanded

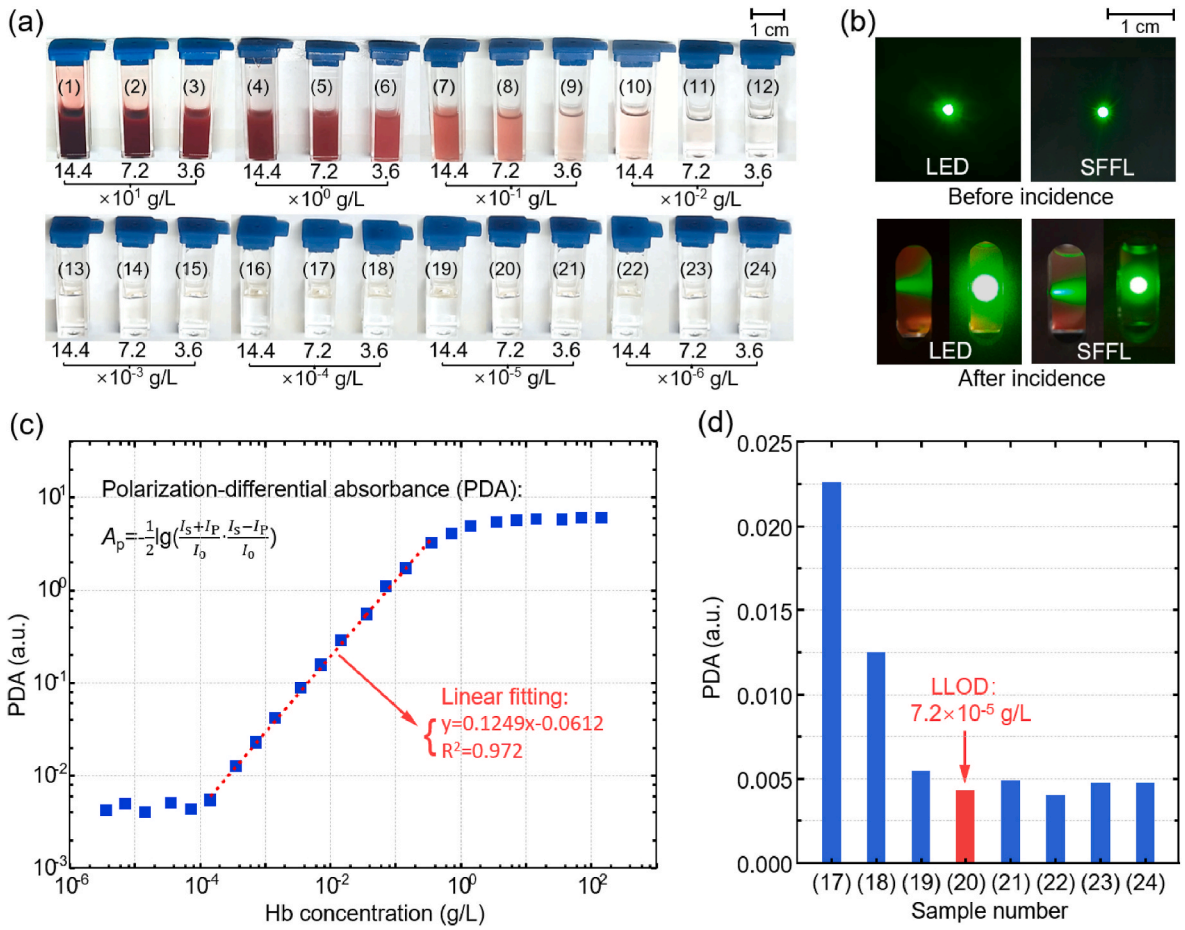

Fig. 4. Hb detection in normal saline based on polarization-differential spectrophotometry. (a) Venous blood samples with different dilution ratios by normal saline. (b) Transmission images based on LED and SFFL as detection light sources for blood samples in normal saline. (c) Hb concentration detection. (d) LLOD of Hb.

tenfold compared to traditional spectrophotometry. Due to the complexity of whole blood samples, the detection linear range of whole blood is often slightly unsatisfactory. Fortunately, our experimental results have made a breakthrough to some extent with the bottleneck of the detection linear range. When Hb concentration is above 3.60×10^{-1} g/L, the absorption characteristic has changed and deviated from the linear interval, which can be ascribed to the decrease in the average distance of the molecules and the influence of the intermolecular charge distribution interaction (Wang et al., 2019). Moreover, the higher the concentration, the farther the deviation, and finally has converged to the upper limit of the detection concentration (14.40 g/L). After that, the detection values show irregular fluctuations. Similarly, when the concentration is below 1.44×10^{-4} g/L, A_P starts to deviate from the linear interval. The PDA decreases as the Hb concentration c decreases, and the value of PDA begins to deviate from the linear relationship at concentrations as low as 1.44×10^{-4} g/L, but is still on a decreasing trend. When the concentration is reduced to 7.2×10^{-5} g/L, the PDA begins to fluctuate up and down, and no useful information about the concentration could be extracted, so the cut-off point is regarded as the LLOD [Masson, 2020; Huang et al., 2013]. The LLOD is demonstrated from the comparison of absorbance values of low-concentration samples in Fig. 4 (d). Regarding the low-concentration sample, the number of red blood cells per unit volume of normal saline is too small to interact evenly with the probe light, causing the detection signal to fluctuate, which limits the further reduction of LLOD.

3.3. Accuracy and repeatability testing

Although the linear fitting is well to characterization, it still exists a certain deviation, especially in terms of accuracy testing. Concerning this issue, polynomial fitting correction, as a common method for multi-influence factors, is adopted to further reduce deviation (Costa et al., 2011). A second-order polynomial fitting of Hb concentration and PDA (C-A_p) is given in Fig. 5(a), and this correlation coefficient has reached 0.999, which is quite superior to the linear fitting correlation coefficient of 0.972. To verify the detected accuracy of Hb concentration, we have conducted comparative experiments between the commercial analytical instrument (Mindray BC-6800Plus) in the Hospital and this experimental system. Before monitoring with our experimental system, we first dilute the blood sample of the volunteer. Then the PDA value of the sample is measured and substituted into the expression to obtain the dilution concentration value C_0. Finally, C_0 is multiplied by the dilution factor to obtain the Hb concentration test value of the volunteer. Based on the collected blood samples from volunteers, 10 groups of detected data coming from the two approaches are very close, as shown intuitively in Fig. 5(b). MRE of the concentration obtained by the C-A_p expression is 3.19%, indicating that this experimental system has comparable accuracy for Hb detection.

The experimental samples with the same Hb concentration are tested seriatim to validate the repeatability. Fig. 5(c) shows the relative standard deviation (RSD) of 10 tests on the same sample (RSD = 1.37%) and ten different samples of the same diluted Hb concentration (RSD = 2.74%). The changes in the results confirm that the measurement data are closely distributed and stable, and have good repeatability. Compared with the ten test results of the same sample, ten different samples with the same diluted Hb concentration introduced deviation caused by the cuvette itself, but the test results are still relatively stable.

To further illustrate the long-term reliability of post-sampling

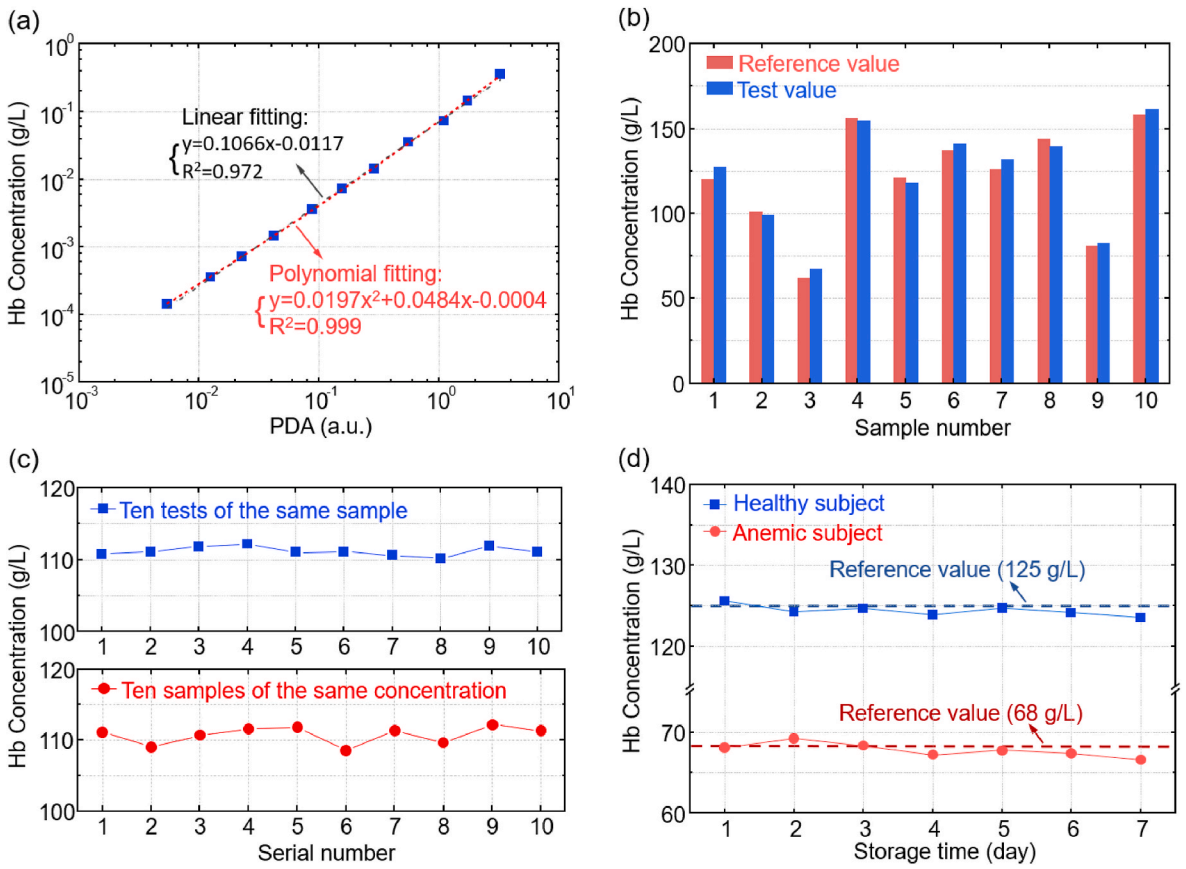

Fig. 5. Accuracy and repeatability testing of Hb detection. (a) Curve *C-A*$_P$ of the blood sample diluted by normal saline. (b) Accuracy testing of Hb concentration in blood samples from 10 volunteers. (c) Repeatability testing. (d) Long-term reliability test results of Hb concentration of healthy and anemic subject.

results, we measure Hb concentration within 7 days after sampling. The biological properties of blood samples usually do not alter too much for a relatively long time at a low temperature of 4 °C (Wong et al., 2017), so this temperature is chosen to store the blood samples. Fig. 5(d) describes changes in the Hb concentration test value of the healthy subject and the anemic subject with the increasing storage days. The deviation of Hb test values from the reference values for the first seven days is minimal with only a small decrease starting on the fifth day, which confirms the long-term reliability of the detection results and the detection repeatability in practical medical applications.

3.4. Comparative analysis

Compared with conventional spectrophotometry, the superiority of polarization-differential spectrophotometry includes: (a) superior detection sensitivity of Hb, which can be used to assist in the early diagnosis of cancer and tumors and as a criterion biosensor for the photometric-based Hb detector; (b) accurately avoid the disadvantage of single signal interference, which has potential to distinguish rare blood disorder with essentially-unchanged Hb concentration.

The comparison of performance indicators of Hb detection techniques is shown in Table 1. For the dynamic range, sensitivity, and linear interval of Hb detection, polarization-differential spectrophotometry has overall advanced by two orders of magnitude compared to conventional spectrophotometry. The sensitivity of polarization-differential spectrophotometry is close to that of fluorescent analysis or electrochemical analysis. Delightingly, polarization-differential spectrophotometry, as an optical detection strategy, has non-destructive effect on the sample, and does not require preprocessing. The time consumption of polarization-differential spectrophotometry is only <10 ms, which will greatly promote the detection efficiency of Hb.

Table 1
Performance indicators of Hb detection techniques.

Performance indicators	Fluorescent analysis (Yang et al., 2017)	Electrochemical analysis (Han et al., 2019)	Spectrophotometry (Fiedoruk-Pogrebniak et al., 2018)	Polarization-differential spectrophotometry
Dynamic range (g/L)	/	/	6.0×10^{-3}~60.0	7.2×10^{-5}~14.4
Sensitivity (g/L)	5.8×10^{-6}	3.0×10^{-5}	6.0×10^{-3}	7.2×10^{-5}
Linear interval (g/L)	1.6×10^{-5}~ 4×10^{-3}	1.0×10^{-4} ~1.0	0.5–30.0	1.4×10^{-4}~ 3.6×10^{-1}
Non-destructive samples	Not	Not	Yes	Yes
Require preprocessing	Yes	Yes	No	No
Time consumption	>12 h	1 h	/	<10 ms

4. Conclusion

To conclude, we demonstrate high-sensitivity Hb detection based on polarization-differential spectrophotometry, and laser intensity variation caused by Hb absorption and polarization state variation owing to Hb anisotropic absorption is considered comprehensively. Benefiting from the combination of two-dimensional information and the superior performance of the self-made 541.5 nm SFFL source, the LLOD of 7.20×10^{-5} g/L and the responsive dynamic range of about six orders of magnitude are obtained for Hb detection. Apart from this, the high accuracy and repeatability of the detection results also confirm the reliability of the test method and the system.

Given the foregoing, the polarization-differential spectrophotometry along with 541.5 nm SFFL holds the following potential benefits: (1) High sensitivity and accuracy can achieve the detection of trace Hb in special parts of the body, which can help medical researchers in the early detection of diseases such as cancer, tumors and organic injuries. (2) The Hb concentration of mild hereditary anemia caused by gene defects (such as thalassemia (Merola et al., 2016) and hereditary stomatocytosis (Risinger and Kalfa, 2020)) is almost normal, while the red blood cells have appeared pathologically abnormal, which suggests invalid diagnosis by means of detecting light intensity changes due to Hb absorption singularly. Our initiative to harness two-dimensional information (i.e., PDA) is expected to realize the diagnosis of the above abnormal blood lesions in time. (3) All signal acquisition processes are completed simultaneously based on compact device, which is easy to operate, practical and reliable. (4) Optically direct detection method means virtually no artificial damage to the blood sample, and does not affect subsequent tests.

In the current experimental setup, we have optimized the detection method and device, and achieved high-sensitivity detection in the experimental stage, but further research and improvement are needed in the following aspects: (1) Part of the experimental apparatus is composed of space optical components, and the anti-shock and anti-disturbance properties cannot be guaranteed. If penetrating into next research and application, the device needs to be integrated to facilitate relocation. (2) The above benefits of this method in medical diagnosis have been confirmed only at the experimental level, and it would be better if the subsequent research could be combined with some specific diseases for more practical and concrete verification.

CRediT authorship contribution statement

Chunlan Deng: conceived the idea and designed experiments, optimized detection device, processed the experimental data and conducted the theoretical analysis, wrote the manuscript. **Qilai Zhao:** Supervision, conceived the idea and designed experiments, optimized detection device, wrote the manuscript, supervised the project. **Yichuan Gan:** assisted in sample processing. **Changsheng Yang:** designed the SFFL source. **Hongbo Zhu:** discussed and commented on the manuscript. **Shiman Mo:** wrote the manuscript. **Junjie Zheng:** designed the SFFL source. **Jialong Li:** optimized detection device. **Kui Jiang:** optimized detection device. **Zhouming Feng:** designed the SFFL source. **Xiaoming Wei:** discussed and commented on the manuscript. **Qinyuan Zhang:** processed the experimental data and conducted the theoretical analysis. **Zhongmin Yang:** Supervision, supervised the project. **Shanhui Xu:** Supervision, supervised the project, All authors revised the manuscript.

Declaration of competing interest

The authors declare that they have no known competing financial interests or personal relationships that could have appeared to influence the work reported in this paper.

Data availability

The authors do not have permission to share data.

Acknowledgments

Work presented in this paper is supported by the National Key Research and Development Program of China (2022YFB3606400), Key-Area Research and Development Program of Guangdong Province (2020B090922006), Major Program of the National Natural Science Foundation of China (61790582), NSFC (12204180, U22A6003, 62275082, 62035015), Fundamental Research Funds for the Central Universities (D6223090), Leading Talents of Science and Technology Innovation of Guangdong Special Support Plan Program (2019TX05Z344), China Postdoctoral Science Foundation (2021M701256), Young Talent Support Project of Guangzhou Association for Science and Technology (QT-2023-053), Guangdong Basic and Applied Basic Research Foundation (2022A1515012594 and 2023A1515010981), Local Innovative and Research Teams Project of Guangdong Pearl River Talents Program (2017BT01X137), Guangzhou Basic and Applied Basic Research Foundation (202201010003), and Open Project Program of Shanxi Key Laboratory of Advanced Semiconductor Optoelectronic Devices and Integrated Systems (2022SZKF02).

References

Amiri, P., DeCastro, J., Littig, J., Lu, H., Liu, C., Conboy, I., Aran, K., 2021. Adv. Sci. 8, e2101912.
Arslanov, D.D., Spunei, M., Mandon, J., Cristescu, S.M., Persijn, S.T., Harren, F.J.M., 2012. Laser Photon. Rev. 7, 188–206.
Baugh, L.M., Liu, Z., Quinn, K.P., Osseiran, S., Evans, C.L., Huggins, G.S., Hinds, P.W., Black, L.D., Georgakoudi, I., 2017. Nat. Biomed. Eng. 1, 914–924.
Costa, K.D., Kleinstein, S.H., Hershberg, U., 2011. Sci. Signal. 4, tr9-tr9.
Dai, H., Yin, C., Ye, X., Jiang, B., Ran, M., Cao, Z., Chen, X., 2017. Sci. Rep. 7, 1–6.
Das, A.J., Wahi, A., Kothari, I., Raskar, R., 2016. Sci. Rep. 6, 1–8.
Dell'Olio, F., Su, J., Huser, T., Sottile, V., Cortés-Hernández, L.E., Alix-Panabières, C., 2021. Laser Photon. Rev. 15, 2000255.
Dremin, V., Zherebtsov, E., Bykov, A., Popov, A., Doronin, A., Meglinski, I., 2019. Appl. Opt. 58, 9398–9405.
Eissa, S., Zourob, M., 2017. Sci. Rep. 7, 1016.
Epah, J., Gülec, I., Winter, S., Dörr, J., Geisen, C., Haecker, E., Link, D., Schwab, M., Seifried, E., Schäfer, R., 2022. Adv. Sci. 9, 2204077.
Fiedoruk-Pogrebniak, M., Granica, M., Koncki, R., 2018. Talanta 178, 31–36.
Han, G.-C., Su, X., Hou, J., Ferranco, A., Feng, X.-Z., Zeng, R., Chen, Z., Kraatz, H.-B., 2019. Sens. Actuators B-Chem. 282, 130–136.
He, C., He, H., Chang, J., Chen, B., Ma, H., Booth, M., 2021. Light Sci. Appl. 10, 194.
Heil, J., Olsavszky, V., Busch, K., Klapproth, K., de la Torre, C., Sticht, C., Sandorski, K., Hoffmann, J., Schönhaber, H., Zierow, J., Winkler, M., Schmid, C.D., Staniczek, T., Daniels, D.E., Frayne, J., Metzgeroth, G., Nowak, D., Schneider, S., Neumaier, M., Weyer, V., Groden, C., Gröne, H.-J., Richter, K., Mogler, C., Taketo, M.M., Schledzewski, K., Géraud, C., Goerdt, S., Koch, P.-S., 2021. Nat. Commun. 12, 6963.
Huang, S., Wang, T., Yang, M., 2013. Assay Drug Dev. Technol. 11, 35–43.
Jian, X., Felsenfeld, G., 2021. Nat. Commun. 12, 4338.
Kalluri, R., LeBleu, V.S., 2020. Science 367, eaau6977.
Kim, J.G., Xia, M., Liu, H., 2005. IEEE Eng. Med. Biol. Mag. 24, 118–121.
Kowalczyk, A., Krajczewski, J., Kowalik, A., Weyher, J., Dzięcielewski, I., Chłopek, M., Góźdź, S., Nowicka, A., Kudelski, A., 2019. Biosens. Bioelectron. 132, 326–332.
Langford, V.S., McKinley, A.J., Quickenden, T.I., 2001. J. Phys. Chem. A 105, 8916–8921.
Lee, Z., Hu, C., Shang, S., Du, K., Lewis, M., Arnone, R., Brewin, R., 2013. J. Geophys. Res. Oceans 118, 4241–4255.
Månberg, A., Skene, N., Sanders, F., Trusohamn, M., Remnestål, J., Szczepińska, A., Aksoylu, I.S., Lönnerberg, P., Ebarasi, L., Wouters, S., Lehmann, M., Olofsson, J., von Gohren Antequera, I., Domaniku, A., De Schaepdryver, M., De Vocht, J., Poesen, K., Uhlén, M., Anink, J., Mijnsbergen, C., Vergunst-Bosch, H., Hübers, A., Kläppe, U., Rodriguez-Vieitez, E., Gilthorpe, J.D., Hedlund, E., Harris, R.A., Aronica, E., Van Damme, P., Ludolph, A., Veldink, J., Ingre, C., Nilsson, P., Lewandowski, S.A., 2021. Nat. Mad. 27, 640–646.
Masson, J.F., 2020. ACS Sens. 5, 3290–3292.
Merola, F., Memmolo, P., Miccio, L., Savoia, R., Mugnano, M., Fontana, A., D'Ippolito, G., Sardo, A., Iolascon, A., Gambale, A., Ferraro, P., 2016. Light Sci. Appl. 6, e16241-e16241.
Miao, X., Yan, L., Wu, Y., Liu, P.Q., 2021. Light Sci. Appl. 10, 5.
Mimee, M., Nadeau, P., Hayward, A., Carim, S., Flanagan, S., Jerger, L., Collins, J., McDonnell, S., Swartwout, R., Citorik, R.J., Bulović, V., Langer, R., Traverso, G., Chandrakasan, A.P., Lu, T.K., 2018. Science 360, 915–918.
Mu, T., Zhang, C., Ren, W., Jia, C., 2012. Opt. Lett. 37, 3507–3509.

Pasricha, S.-R., Tye-Din, J., Muckenthaler, M.U., Swinkels, D.W., 2021. Lancet 397, 233–248.
Passos, L.C., Saraiva, M.M.F.S., M, L., 2019. Measurement 135, 896–904.
Pillai, A.S., Chandler, S.A., Liu, Y., Signore, A.V., Cortez-Romero, C.R., Benesch, J.L.P., Laganowsky, A., Storz, J.F., Hochberg, G.K.A., Thornton, J.W., 2020. Nature 581, 480–485.
Ra, Y.-H., Rashid, R.T., Liu, X., Sadaf, S.Md., Mashooq, K., Mi, Z., 2020. Sci. Adv. 6, eaav7523.
Risinger, M., Kalfa, T.A., 2020. Blood 136, 1250–1261.
Ryu, W.-H., Gittleson, F.S., Thomsen, J.M., Li, J., Schwab, M.J., Brudvig, G.W., Taylor, A. D., 2016. Nat. Commun. 7, 12925.
Sereda, A., Moreau, J., Canva, M., Maillart, E., 2013. Biosens. Bioelectron. 54, 175–180.
Shuhang, T., Shi, Z., Sun, Y., Zhang, P., Wu, S., Chen, D., Xiong, P., Qian, Q., Yang, Z., 2022. Laser Photon. Rev. 16, 2200020.
Suhito, I.R., Kim, J.W., Koo, K., Nam, S.A., Kim, Y.K., Kim, T., 2022. Adv. Sci. 9, 2200074.
Tenner, B., Zhang, J.Z., Kwon, Y., Pessino, V., Feng, S., Huang, B., Mehta, S., Zhang, J., 2021. Sci. Adv. 7, eabe4091.
Veenstra, C., Kruitwagen, S., Groener, D., Petersen, W., Steenbergen, W., Bosschaart, N., 2019. Sci. Rep. 9, 15115.
Venables, S.V., Drerup, C., Powell, S.B., Marshall, N.J., Herbert-Read, J.E., How, M.J., 2022. Sci. Adv. 8, eabq2770.
Vlk, M., Datta, A., Alberti, S., Yallew, H.D., Mittal, V., Murugan, G.S., Jágerská, J., 2021. Light Sci. Appl. 10, 26.
Wang, T., Lv, H., Huang, J., Shan, H., Feng, L., Mao, Y., Wang, J., Zhang, W., Han, D., Xu, Q., Du, P., Zhao, A., Wu, X., Tait, S.L., Zhu, J., 2019. Nat. Commun. 10, 4122.
Wong, K.H.K., Tessier, S.N., Miyamoto, D.T., Miller, K.L., Bookstaver, L.D., Carey, T.R., Stannard, C.J., Thapar, V., Tai, E.C., Vo, K.D., Emmons, E.S., Pleskow, H.M., Sandlin, R.D., Sequist, L.V., Ting, D.T., Haber, D.A., Maheswaran, S., Stott, S.L., Toner, M., 2017. Nat. Commun. 8, 1733.
Wyatt, J.S., Delpy, D.T., Cope, M., Wray, S., Reynolds, E.O.R., 1986. Lancet 328, 1063–1066.
Xu, S., Yang, Z., Zhang, W., Wei, X., Qian, Q., Chen, D., Zhang, Q., Shen, S., Peng, M., Qiu, J., 2011. Opt. Lett. 36, 3708–3710.
Yakushiji, F., Yakushiji, K., Murata, M., Hiroi, N., Fujita, H., 2021. Hematol. Transfus. Int. J. 9, 5–10.
Yang, D., Meng, H., Tu, Y., Yan, J., 2017. Talanta 170, 233–237.
Zhao, X., Lu, D., Liu, Q.S., Li, Y., Feng, R., Hao, F., Qu, G., Zhou, Q., Jiang, G., 2017. Adv. Sci. 4, 1700296.
Zhou, Y., Arribas, G.H., Turku, A., Jürgenson, T., Mkrtchian, S., Krebs, K., Wang, Y., Svobodova, B., Milani, L., Schulte, G., Korabecny, J., Gastaldello, S., Lauschke, V.M., 2021. Sci. Adv. 7, eabi6856.
Zou, S., Li, P., Wang, L., Chen, M., Li, G., 2009. Appl. Phys. B 95, 685–690.